Brain Research 1782 (2022) 147837

Contents lists available at ScienceDirect

Brain Research

journal homepage: www.elsevier.com/locate/brainres

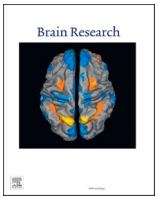

A_{2B} adenosine receptor inhibition ameliorates hypoxic-ischemic injury in neonatal mice via PKC/Erk/Creb/HIF-1α signaling pathway

Junyan Wang [a], Dan Wang [a], Xiaomin Zheng [b], Yunhong Li [a], Yilu Li [a], Teng Ma [a], Jinxia Li [a], Jinping Sun [a], Yin Wang [a,*], Quanrui Ma [a,*]

[a] School of Basic Medicine, Ningxia Medical University, Yinchuan 750004, Ningxia, PR China
[b] Department of Pediatric Neurorehabilitation, People's Hospital of Ningxia Hui Autonomous Region, Yinchuan 750004, PR China

ARTICLE INFO

Keywords:
A_{2B} adenosine receptor
Hypoxia-Ischemia
Periventricular leukomalacia
Hypomyelination
Neuroinflammation

ABSTRACT

Periventricular leukomalacia (PVL), the dominant cerebral white matter injury disease, is induced by hypoxia–ischemia and inflammation in premature infants. The activation of A_{2B} adenosine receptor (A_{2B}AR) is shown to involve into inflammation, ischemia, and other typical stress reactions, but its exact function in PVL has not been clarified. We gained initial insight from PVL mouse model (P9) by the induction of hypoxia–ischemia with right carotid ligation followed by exposure to hypoxia and intraperitoneal (i.p.) injection of Lipopolysaccharide (LPS). The results showed that treatment of PSB-603, an A_{2B}AR selective antagonist, greatly ameliorated cerebral ischemic injury by increasing body weights, reducing infarct volume, brain injury, inflammation and contributing to long-term learning memory functional recovery of the PVL mice. Meanwhile, PSB-603 treatment suppressed neurons apoptosis as characterized by reducing of Caspase-3 level, inhibited microglia activation and attenuated hypomyelination through promoting MBP expression and oligodendrocytes differentiation. A_{2B}AR inhibition also augmented PKC expression, the activity of PKC downstream signaling molecules were then explored. Erk expression and Creb phosphorylation exhibited upregulation in PSB-603 treatment group compared with the control group. Hypoxia Inducible Factor-1α (HIF-1α), a direct target of hypoxia, which is a key regulator of adenosine signaling by binding to the A_{2B}AR promoter to induce expression of A_{2B}AR, was shown to be decreased by PSB-603. Taken together, A_{2B}AR inhibition can ameliorate hypoxic-ischemic injury in PVL mice maybe through PKC/Erk/Creb/HIF-1α signaling pathway.

1. Introduction

Periventricular leukomalacia (PVL) is a high mortality and morbidity disease with a profound impact on motor, cognitive sensory and social development, which is identified as the most severe danger for very premature brains of infants characterized by the injury and differentiation block of oligodendrocyte progenitor cells (OPC) in the periventricular white matter caused by the ischemia, hypoxia and infection, resulting in the failure of myelinogenesis (Haynes and van Leyen, 2013). At present, therapeutic approaches for infants suffering from PVL injury are mainly symptomatic. Therefore, it is necessary to explore novel therapies to prevent or treat brain injury of PVL.

Adenosine, a naturally occurring nucleoside, also a ubiquitous neuromodulator, slows down inflammation in various disease models by activating its four G-protein-coupled receptors termed A_1AR, A_{2A}AR, A_{2B}AR and A_3AR (Verkhratsky and Burnstock, 2014; Liu et al., 2017). In the event of stress and injury, especially under pathological conditions such as ischemia, hypoxia and inflammation, the level of adenosine increases abnormally (200 times that under physiological conditions) (Montalbán del Barrio et al., 2016). Its receptor A_{2B}AR is rarely

Abbreviations: PVL, Periventricular leukomalacia; A_{2B}AR, adenosine receptor A_{2B}; P9, postnatal day 9; i.p, intraperitoneal; LPS, Lipopolysaccharide; PSB, A_{2B}AR selective antagonists PSB-603; BAY, A_{2B}AR selective agonists BAY60-6583; PKA, protein kinase A; PKC, protein kinase C; Erk, extracellular regulated protein kinases; Creb, cAMP-response element binding protein; P-Creb, phosphor-cAMP-response element binding protein; HIF-1α, hypoxia inducible factor-1α; CNS, central nervous system; Caspase-3, Cysteinyl aspartate-selective proteinase-3. NeuN, neuronal nuclei antigen; CC-1, adenomatous polyposis coli; Olig2, Oligodendrocyte lineage transcription factor 2; OPC, oligodendrocyte progenitor cells; TNF-α, tumour necrosis factor-α; IL-6, interleukin-6; IL-1β, interleukin-1β; IL-10, interleukin-10; Iba-1, ionized calcium binding adapter; DI, discrimination index; PI, preference index.

* Corresponding authors at: School of Basic Medical Sciences, Ningxia Medical University, Yinchuan 750004, PR China.
E-mail addresses: wang@hotmail.com (Y. Wang), Maqr220080808@163.com (Q. Ma).

https://doi.org/10.1016/j.brainres.2022.147837
Received 20 November 2021; Received in revised form 12 February 2022; Accepted 14 February 2022
Available online 16 February 2022

distributed in the central nervous system, but it is found that A_{2B}AR participates in pathophysiological processes with extremely important physiological significance for it is activated by the release of higher concentration of adenosine only in the case of tissue injury (Lindemann et al., 2020; Gnad et al., 2020); indicating that A_{2B}AR may be a possible therapeutic target for PVL. A_{2B}AR is coupled to a variety of signaling pathways, of which the Gq-phospholipase C (PLC)-protein kinase C (PKC) pathway is the most typical (Schulte and Fredholm, 2003).

In the present study, a periventricular leukomalacia (PVL) animal model was established with right carotid ligation followed by exposure to hypoxia and intraperitoneal (i.p.) injection of LPS and treated with A_{2B}AR selective antagonist PSB-603. The protective role of A_{2B}AR inhibition in PVL mice was primarily observed. Furthermore, the mechanism of A_{2B}AR inhibition ameliorating hypoxic-ischemic injury in PVL mice through PKC/Erk/Creb/HIF-1α signaling pathway was explored.

2. Results

2.1. Hypoxia-ischemia with LPS impaired myelination in developing brains of mice

To determine whether the animal model of LPS combined with hypoxia–ischemia was a reasonable model to simulate prenatal infant white matter injury, we used right carotid artery ligation combined with hypoxia exposure (8% oxygen) to induce ischemia and hypoxia, followed by LPS injection on newborn mice at postnatal day 9. This age corresponds exactly to weeks 32–40 of human pregnancy (Ortega et al., 2016). The weights of the mice in all groups were almost similar at the beginning of the study. After PVL, from the 9th day to the 14th day, the body weights of the mice in the PVL model group were significantly reduced compared with those of the control group (Fig. 1B). At P14, myelin sheath in the brain was examined by immunofluorescence staining for myelin basic protein (MBP), and the MBP expression was significantly reduced in white matter on the ipsilateral side of brain in PVL (Fig. 1C-D). The protein expression level of MBP was also significantly reduced in the mouse brain of the PVL group compared with normal littermates (**$P < 0.01$) (Fig. 1E-F). These results showed that hypoxia–ischemia with LPS inhibited myelination in the developing CNS of PVL mice.

2.2. Blocking of A_{2B}AR with PSB-603 attenuated cerebral white matter injury in mice with PVL

To explore the effects of A_{2B}AR on white matter damage in the PVL

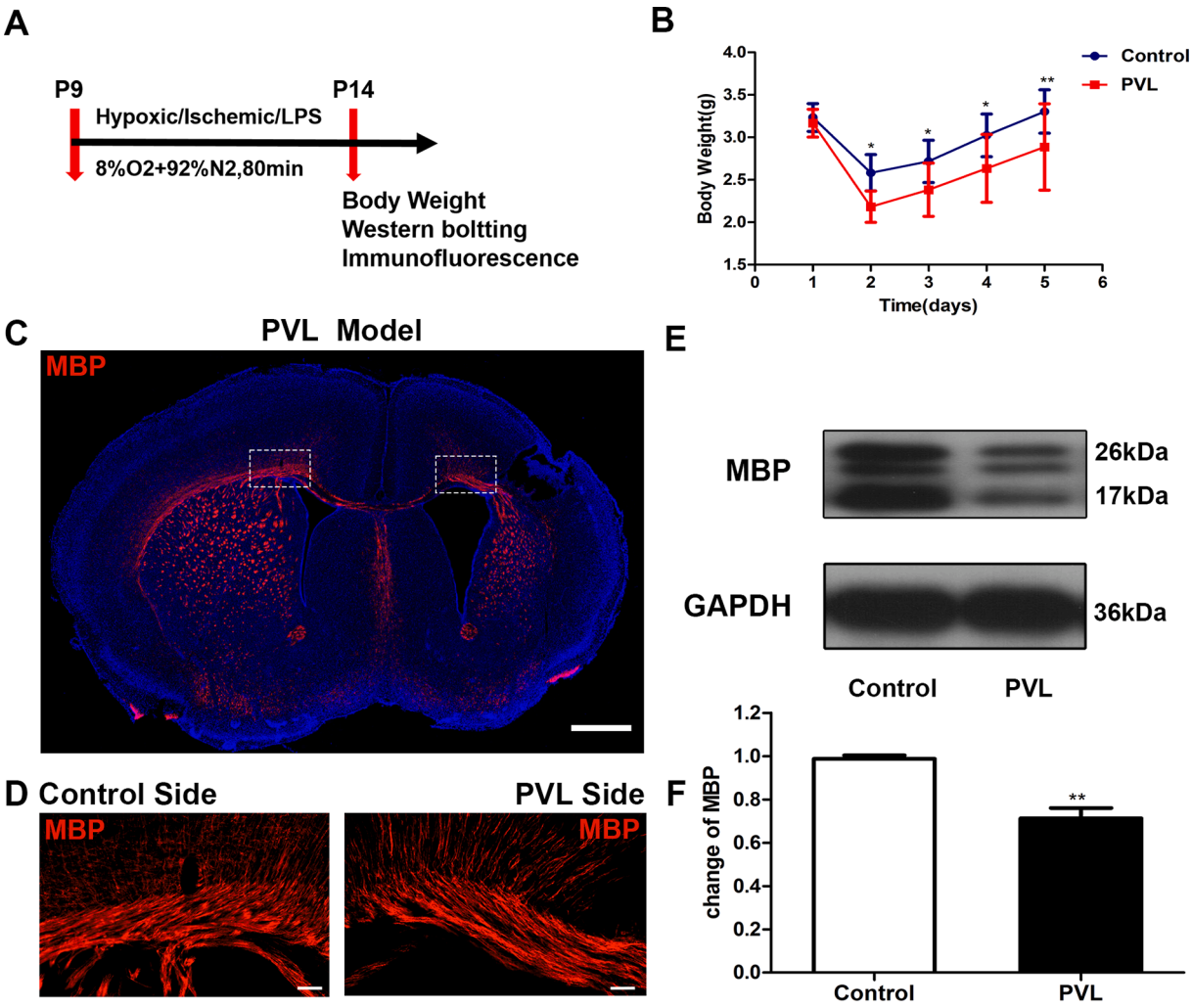

Fig. 1. Hypoxia-ischemia with LPS results in hypomyelination in neonatal mice. (A) The process of model and analysis. (B) Changes in the body weights in 5 days of PVL modeling. (C) Representative immunofluorescent images displaying a dramatic reduction of MBP-positive fibers in the brains of PVL mice. (D) Enlarged images showing MBP-positive fibers in the corpus callosum (The left picture represents normal; The right picture represents damage). Scale bar = 1 mm (C) and Scale bar = 50 μm (D). (E) Representative western blotting images of MBP and the analysis of MBP protein expression levels in the right cortex. All data are expressed as the mean ± SD (n = 5). **$P < 0.01$, vs. the PVL group. PVL, Periventricular leukomalacia; MBP, myelin basic protein.

mouse model, the mouse was treated with a single i.p. injection of $A_{2B}AR$ selective antagonist PSB-603 (25 μg/kg/d, i.p.) and agonist BAY60-6583 (80 μg/kg/d, i.p.) or an equal amount of saline immediately after PVL (Fig. 2A). Similar body weights were recorded for all groups at the start of the study, but after treatment, there were remarkable differences in the body weights between the PVL group and PVL + PSB group at P14 (Fig. 2B). Interestingly, the olfactory discrimination decreased in the PVL + PSB group compared with PVL group (*$P < 0.05$) (Fig. 2C). The brain insult was assessed by infarct staining with TTC at P14 showing that the infarct area was mainly located in the cortex and corpus callosum of the right hemisphere. Compared with the sham group, the cerebral infarct area in the PVL group was significantly larger. The infarct size decreased significantly after PSB-603 treatment compared with the PVL group (***$P < 0.001$), but there was no significant difference between PVL group and PVL + BAY group (Fig. 2D-E). These results indicated that intervention of $A_{2B}AR$ selective antagonist PSB-603 attenuated cerebral white matter injury of the PVL mice, whereas the agonist BAY60-6583 did not ameliorate this degree of damage.

2.3. Blocking of $A_{2B}AR$ with PSB-603 inhibited neuron damage in mice with PVL

To further determine the impacts of $A_{2B}AR$ on PVL-induced neuronal injury in the brain, brain tissues and sections were collected for H&E and Nissl staining (Fig. 3A). In the PVL group, overt signs of neuronal injury were observed in the right cortex. Neuronal tissue disorder, as well as the presence of loose and vacuolated nerve fibers, were accompanied by the disappearance of a large number of nissl bodies in the cytoplasm. However, the extent of such neuronal degeneration and necrosis was significantly reduced and the number of necrotic cells was significantly lower in the PVL + PSB group, but there was no significant difference between the PVL group and the PVL + BAY group (Fig. 3B-D). The

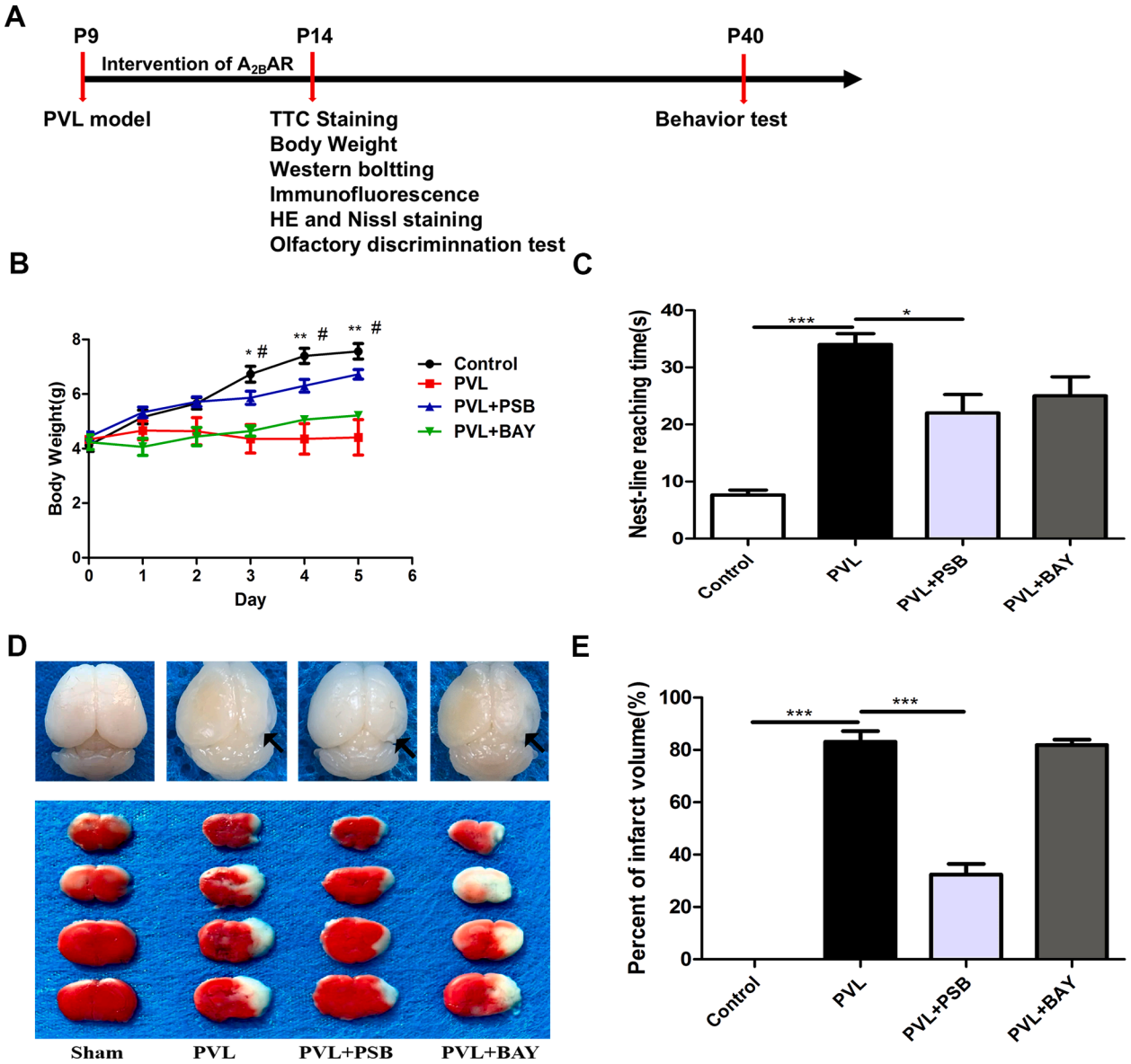

Fig. 2. $A_{2B}AR$ inhibition had a protective effect on brain injury and neurological deficits after PVL. (A) The time course of experiment and assays. (B) Changes in the body weights in 5 days of PVL modelling and 5 days of interventions with selective antagonist or agonist of $A_{2B}AR$(*: PVL vs. Control; #: PVL vs. PVL + PSB). (C) Olfactory discrimination test after interventions with selective antagonist or agonist of $A_{2B}AR$. (D) The black barrows represent damaged areas of brain tissue and representative TTC staining image with a white area showing an ischemic infarct area. (E) The evaluation of infarct size. All data are expressed as the mean ± SD (n = 3–5).*,# P < 0.05, **P < 0.01 and ***P < 0.001 vs. the PVL group. PVL, Periventricular leukomalacia; PSB, $A_{2B}AR$ selective antagonist PSB-603; BAY, $A_{2B}AR$ selective agonist BAY60-6583.

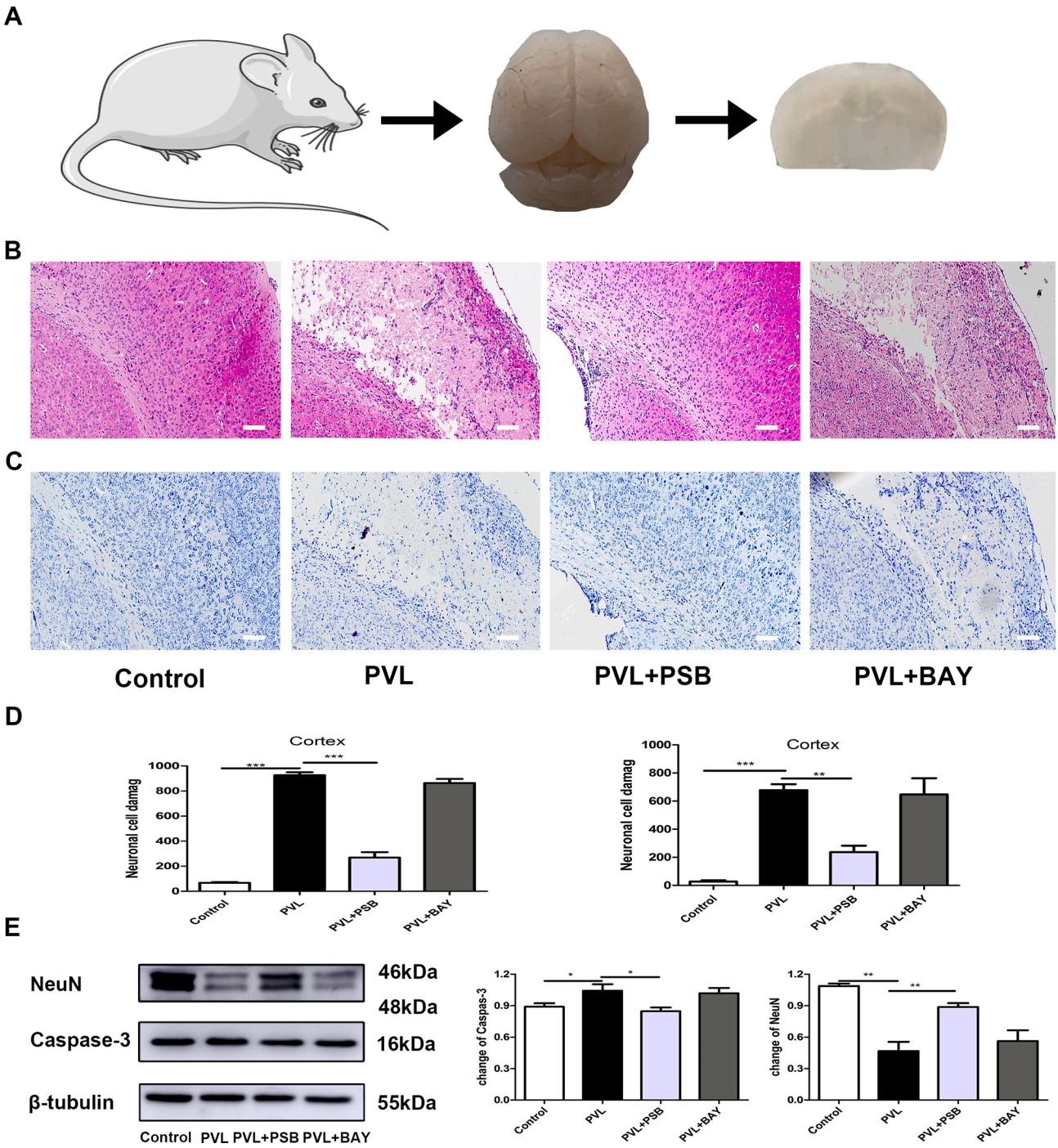

Fig. 3. Influence of A_{2B}AR inhibition on morphology and cell death in the right cortex area. (A) The process of collecting brain tissue and the detected area. (B and C) Representative HE and Nissl staining images of the right ischemic cerebral cortex. Scale bar = 50 μm. (D) The statistical plot of B and C, representing the number of dead neurons in the cerebral cortex. (E) Representative western blotting images of Caspase-3 and NeuN, and the analysis of protein expression level of Caspase-3 and NeuN in the right cortex. All data are expressed as the mean ± SD (n = 3–5). *$P < 0.05$, vs. the PVL model group. PVL, Periventricular leukomalacia; PSB, A_{2B}AR selective antagonist PSB-603; BAY, A_{2B}AR selective agonist BAY60-6583; Caspase-3, Cysteinyl aspartate-selective proteinase-3. NeuN, neuronal nuclei antigen.

protein level of neuronal nuclear antibody (NeuN), which was a neuron marker, was consistent with the Nissl staining results described above (Fig. 3E). There was significant evidence of cell death as measured by increased protein expression level of the cleaved caspase-3 in the PVL group. Conversely, after A_{2B}AR selective antagonist PSB-603 treatment, the expression of caspase-3 was noticeably reduced (*$P < 0.05$) (Fig. 3E). These results indicated that the A_{2B}AR agonist BAY60-6583 did not ameliorate the neuronal damage of the PVL mice, but the intervention of the antagonist PSB-603 significantly alleviated the damage to a certain extent.

2.4. *Blocking of A_{2B}AR with PSB-603 attenuated hypomyelination in mice with PVL*

To further evaluate the effect of A_{2B}AR on myelination in cerebral white matter damage of PVL, the immunofluorescent staining was conducted. The results showed that MBP-positive fibers in the corpus callosum were greatly enhanced in PVL + PSB group compared with that in

the PVL group (Fig. 4A). Western blotting results showed that compared with PVL group, the expression levels of MBP protein in PVL + PSB group and PVL + BAY group were significantly increased. (*$P < 0.05$) (Fig. 4B-C). Meanwhile, immunofluorescent staining showed that differentiated OLs (CC1+/Olig2 +) in the PVL group significantly decreased compared with the Control group in the right cortex (***$P < 0.001$) (Fig. 4D-F). The numbers of CC1+/Olig2+ positive cells in the right cortex and the corpus callosum of the PVL + PSB group were more than that of the PVL group (*$P < 0.05$, **$P < 0.01$). At the same time, it was also observed that the number of CC1+/Olig2 + positive cells in the right cortex the PVL + BAY group was more than that of PVL group (*$P < 0.05$). These results indicated that intervention of PVL by A_{2B}AR selective antagonist PSB-603 and agonist BAY60-6583 attenuated hypomyelination and promoted differentiation of OLs, while the therapeutic effect of agonists is less pronounced than that of antagonists.

2.5. Blocking of A_{2B}AR with PSB-603 alleviated inflammation in mice with PVL

Accumulating evidence has demonstrated that PVL can lead to inflammation or infection. Consistent with the report, inflammatory cytokines IL-6, TNF-α, IL-1β, and IL-10 concentrations in brain tissue of PVL group were significantly higher than those of the control group. As expected, after intervention with PSB-603, these markers were dramatically lower than those in the PVL group (**$P < 0.01$ and ***$P < 0.001$). At the same time, IL-6 and IL-1β were changed in PVL + BAY group compared with PVL group (*$P < 0.05$) (Fig. 5A). In addition, we also observed the morphological changes of microglia through immunofluorescence staining. After PVL, the number of microglia cell protrusions decreased sharply, showing an amoeba-like morphology. However, after PSB-603 intervention this situation had been effectively improved (Fig. 5B). The protein expression level of Iba1 (microglia marker) was greatly increased in the PVL group (*$P < 0.05$) indicating the appearance of inflammation because microglia was a key regulator of inflammatory responses in the CNS. However, the microglia number was decreased after PSB-603 treatment. (*$P < 0.05$) (Fig. 5C). Therefore, intervention of PVL by A_{2B}AR selective antagonist PSB-603 significantly alleviated inflammation in mice with PVL, whereas the agonist BAY60-6583 was less effective in ameliorating inflammation.

2.6. Blocking of A_{2B}AR with PSB-603 promoted myelination and functional recovery in adult mice with PVL

It has been reported that PVL leads to long-term learning and cognitive dysfunction in patients. Next, we investigated whether A_{2B}AR intervention after PVL promoted myelin formation and the recovery of neurological deficits. Since learning and cognitive deficits are also commonly in patients with PVL, the new object recognition tests were performed in this study to evaluate non-spatial learning, recognition and memory functions. The results indicated that the PVL group exhibited a negative DI value. Compared with the sham group, the mice in the PVL group showed significantly reduced ability to explore new objects and reduced preference for new objects, while the mice in the PVL + PSB group showed restored ability to explore new objects and preference (Fig. 6A-D). Collectively, these findings indicated that PVL may decrease the ability of the mouse to recognize and remember new objects and that intervention of A_{2B}AR may repair these deficits. The mice were subjected to the grip strength examination at P40 and the forelimb grip strength scores of PVL group were substantially lower than sham group. On the other hand, PVL group treated by PSB-603 showed drastically ameliorated grip strength test scores (Fig. 6E). Meanwhile, the level of MBP expression in the PVL group was lower than those in the sham group and the PVL + PSB group (Fig. 6F).

2.7. Blocking of A_{2B}AR with PSB-603 attenuated PVL via the PKC/Erk/Creb/HIF-1α signaling pathway.

A_{2B}AR was reported to couple with a variety of signaling pathways. In recent years, research focuses on Gq-phospholipase C (PLC)-protein kinase C (PKC) and MAPK pathway (Schulte and Fredholm, 2003; Salsoso et al., 2021). To further explore the possible neuroprotective molecular mechanism of A_{2B}AR; we detected levels of PKC, extracellular regulated protein kinases (Erk) and cAMP-response element binding protein (Creb) using western blotting analysis. Meanwhile, we examined the level of Hypoxia Inducible Factor-1α (HIF-1α), a direct target of hypoxia and a key regulator of adenosine signaling by binding to the A_{2B}AR promoter induce expression of A_{2B}AR (Kwon et al., 2019). Results showed that hypoxia–ischemia with LPS induced injury decreased PKC, Erk, p-Creb levels in the PVL group (*$P < 0.05$), and increased the expression levels of p-PKC, p-Erk, HIF-1α (*$P < 0.05$ and **$P < 0.01$) (Fig. 7A-B). However, blocking of A_{2B}AR with PSB-603 drastically enhanced PKC, Erk, p-Creb levels and decreased p-PKC, p-Erk, HIF-1α levels in comparison with the PVL group (*$P < 0.05$ and **$P < 0.01$). However, only p-Creb was significantly different between the PVL + BAY group and PVL group (*$P < 0.05$) (Fig. 7A-B). The aforementioned studies demonstrate that intervention of PVL by the A_{2B}AR selective antagonist PSB-603 causes PKC phosphorylation and triggers a signaling cascade via Erk1/2 phosphorylation that may activate Creb and regulate HIF-1α expression. However, treatment with the agonist BAY60-6583 caused only Creb phosphorylation. In summary, these results indicated that the neuroprotective effect of A_{2B}AR inhibition on PVL may be related to the involvement of the PKC/Erk/Creb/HIF-1α.

3. Discussion

The developing cerebral white matter of premature baby is extremely vulnerable to hypoxia, ischemia, infection and inflammation (Back, 2017; Harmony, 2021) The destruction of immune system and infectious inflammation will affect the myelin sheath around axons, thus change the transmission and function of neurons, and eventually lead to the occurrence of nerve injury related diseases (Rumajogee et al., ; Haskó et al., 2008). In the present study, we established a P9 PVL mouse model by ischemia-hypoxia combined with LPS injection to mimic the periventricular leukomalacia, which showed the infarction atrophy and degeneration of nuclei in the ischemic area, as well as demyelination, activation of microglia and learning and cognitive deficits, suggesting the success of the PVL model.

Ischemia and hypoxia affect the energy supply of brain cells in preterm infants. Adenosine, an intermediate for the synthesis of adenosine triphosphate (ATP), is involved in energy metabolism and increases blood flow, which plays an important role in the immune system and inflammation. A_{2B}AR is a subtype of adenosine receptor with low affinity for adenosine and requires high concentration of adenosine released under pathological conditions including ischemia and inflammation (Effendi et al., 2020). Therefore, the use of A_{2B}AR based research therapy has aroused great interest of scientists in the treatment of infection, autoimmunity and ischemia (Franklin and ffrench-Constant, 2017). Here we found that treatment of PVL mice with A_{2B}AR selective antagonist PSB-603 greatly ameliorated cerebral ischemic injury. PSB-603 significantly reduced the cerebral infarction area and alleviated ischemic damage. The HE and Nissl staining results showed the karyopycnosis, neuronal necrosis and inflammatory cell infiltration were increased significantly in PVL mice model, which were greatly improved by intraperitoneal injection of PSB-603. Further results showed that PSB-603 could significantly decrease caspase-3 expression and increase NeuN expression indicating that the blockade of A_{2B}AR can attenuate the injury from PVL mice by reducing neuron apoptosis.

The hallmark of the pathology observed in premature infants of PVL is white matter injury (WMI), which manifests as an arrested development of the oligodendrocytes (OLs) lineage and a subsequent reduction

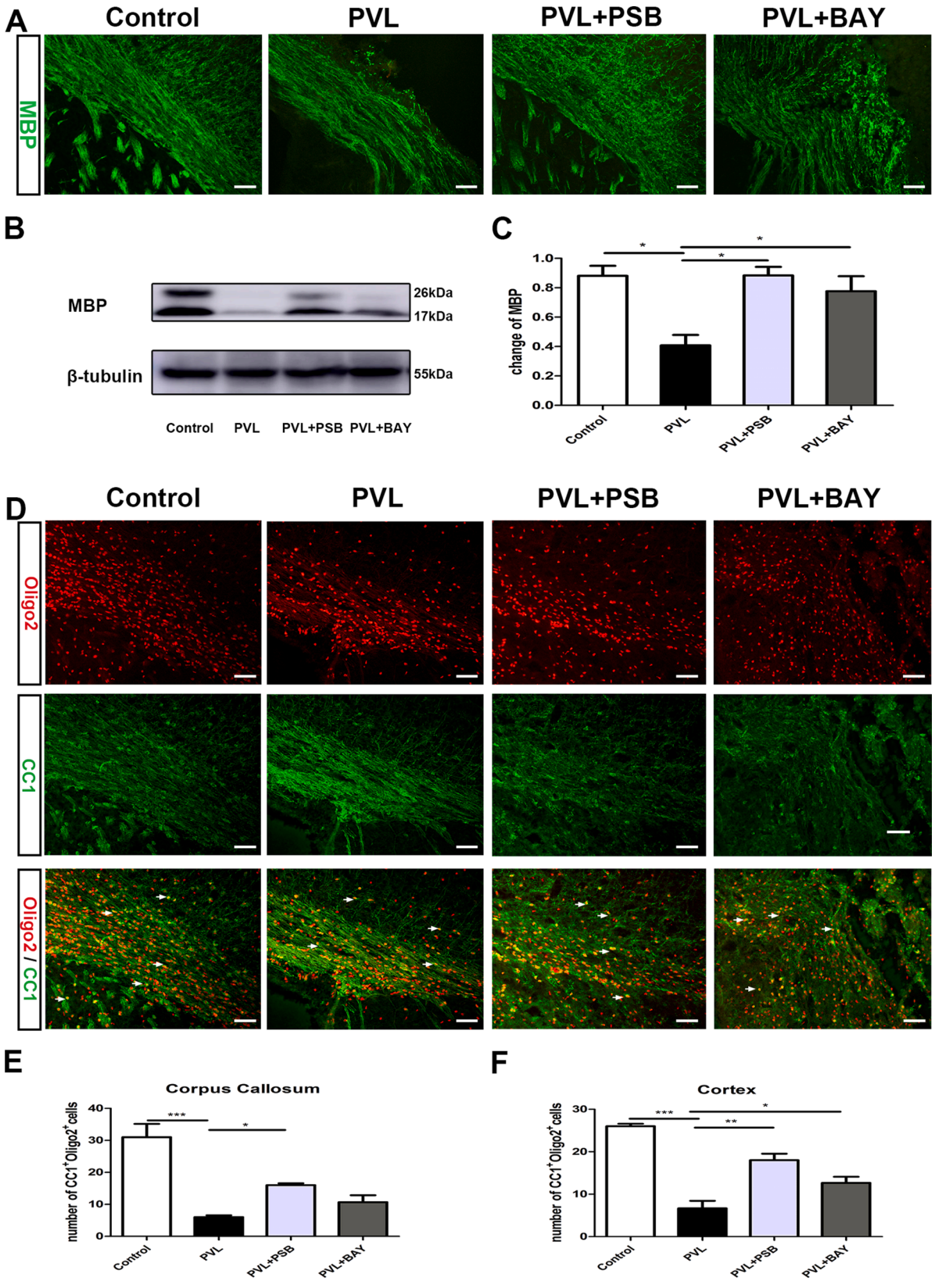

Fig. 4. A_{2B}AR inhibition attenuated hypomyelination in mice with PVL. (A) Representative immunofluorescent images displaying MBP-positive fibers in the corpus callosum of mice. Scale bar = 50 μm. (B-C) Representative western blotting images of MBP and the analysis of MBP protein expression levels in the cortex. (D) Representative immunofluorescent images displaying of differentiated OLs (CC1+/Olig2+ cells indicated by arrows) in the corpus callosum of the brain, green indicated CC-1 positive cells, red indicated Olig2 positive cells. Scale bar = 50 μm. (E-F) Statistical graph of the number of CC1+/Olig2+ positive cells in the corpus callosum and the right cortex of the brain. All data are expressed as the mean ± SD (n = 3–5). $^{*}P < 0.05$, $^{**}P < 0.01$ and $^{***}P < 0.001$ vs. the PVL model group. PVL, Periventricular leukomalacia; MBP, myelin basic protein; CC-1, adenomatous polyposis coli; Olig2, Oligodendrocyte lineage transcription factor 2; PSB, A_{2B}AR selective antagonist PSB-603; BAY, A_{2B}AR selective agonist BAY60-6583.

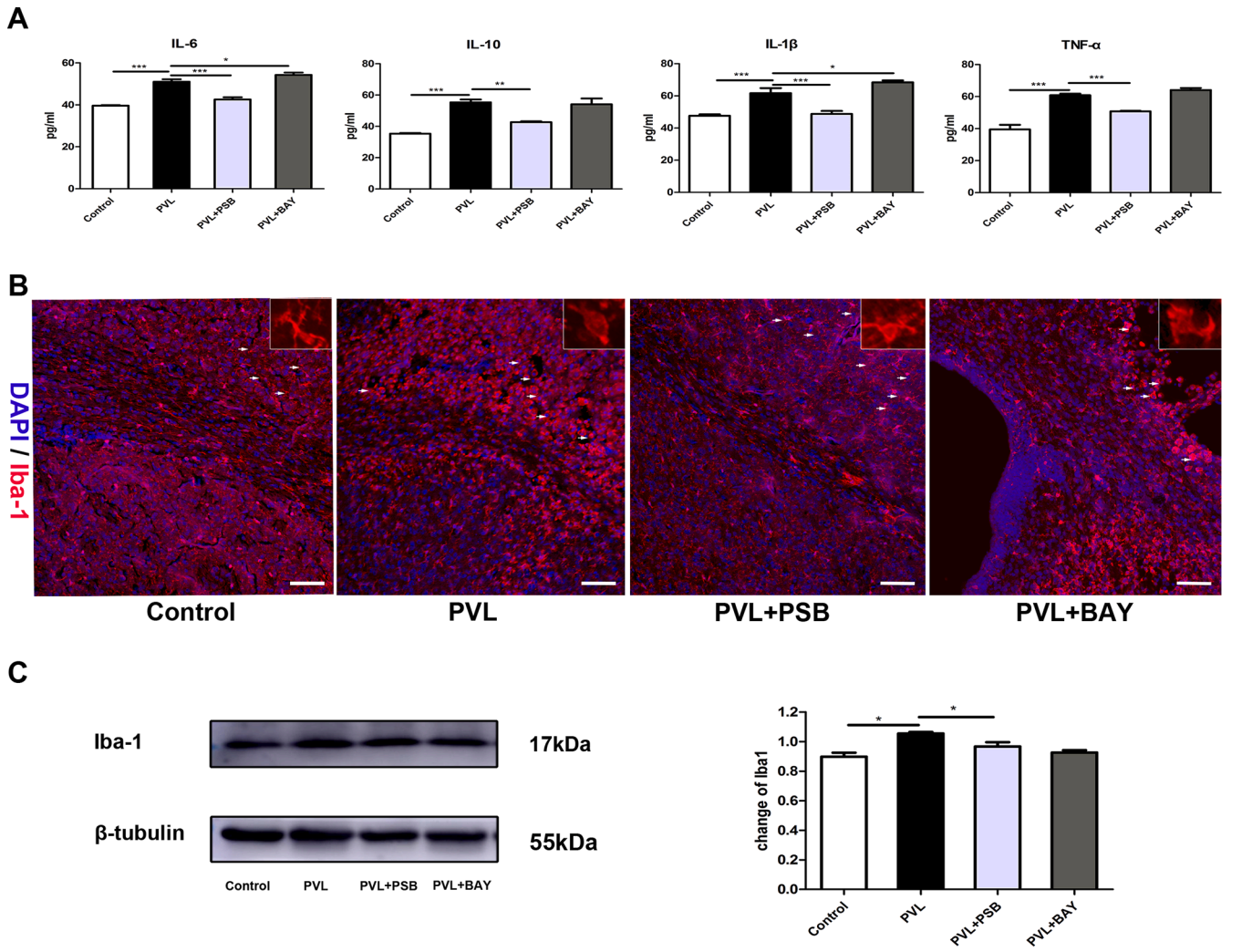

Fig. 5. Effects of A_{2B}AR inhibition on inflammation in PVL model. (A) The levels of TNF-α, IL-1β, IL-6 and IL-10 in the supernatants of brain tissue determined by ELISA kits. (B) Representative immunofluorescent images displaying microglia cell (Iba-1) in the corpus callosum of mice. Scale bar = 100 μm; (C) Representative western blotting images of Iba-1and the analysis of Iba-1 protein expression levels in the cortex. All data are expressed as the mean ± SD (n = 3–5). $^{*}P < 0.05$ $^{**}P < 0.01$ and $^{***}P < 0.001$ vs. the PVL model group. PVL, Periventricular leukomalacia; TNF-α: tumour necrosis factor-α; IL-6: interleukin-6; IL-1β: interleukin-1β; IL-10: interleukin-10; Iba-1, ionized calcium binding adapter; PSB, A_{2B}AR selective antagonist PSB-603; BAY, A_{2B}AR selective agonist BAY60-6583.

in brain myelination (Chang et al., 2016). Demyelination is a major pathological component of WMI that significantly contributes to behavioral and cognitive impairments (Coppi et al., 2020). A_{2B}AR is rarely but widely distributed across neurons and glial cells in the CNS and is reported to play a key role in the development of oligodendrocytes (Simon et al., 2011). We confirmed that the MBP level was remarkably increased after A_{2B}AR blocked with PSB-603 in PVL mice, which suggests that inhibition of A_{2B}AR has obvious protective effects on white matter damage. In most demyelinating disease models, remyelination is hindered mainly because OPC fails to differentiate into mature OLs rather than OPC proliferation or migration failure (Neumann et al., 2019; Mao et al., 2020). In a recently reported article with a disease model similar to this study, it was noted that ischemia-induced GPR17 expression was shown to contribute to glial-derived progenitor cell differentiation into OL precursors, which may provide a therapeutic target for immature neonatal white matter injury after ischemia (Miron et al., 2013). Consistent with this report, we demonstrated that more CC1+/Olig2+ positive cells in PVL brain treated with PSB-603, indicating that the blockade of A_{2B}AR promoted OL maturation and remyelination.

Microglia are macrophages and play a key role in mediating various relevant immune functions (Han et al., 2017). The severity of WMI is reported to be related to the number of pro-inflammatory microglia. In this study, we discovered that PSB-603 significantly decreased the expression of Iba1, one of microglia marker, in PVL model mice. Meanwhile, PSB-603 significantly reversed the production of cytokines TNF-α, IL-1β, and IL-6 in the PVL model. It has been documented that IL-1β and TNF-α produced by microglia in the neonatal rats following LPS exposure may impede OL maturation and impair axonal myelination, which were reversed by treatment with an IL-1β receptor inhibitor (Sherwin and Fern, 2005; Wei et al., 2013). Wei et al. found that knockout A_{2B}AR or blocking A_{2B}AR with selective antagonists could block IL-6 production and Th17 differentiation in CNS and attenuate demyelination in EAE mice (Aherne et al., 2011). Therefore, we speculated that blocking A_{2B}AR may promote OL maturation and remyelination by reducing microglial numbers and the secretion of cytokines. Actually, it cannot be ignored that A_{2B}AR has a wide variety of functions (Fredholm et al., 2011; van der Hoeven et al., 2011); which may render unexpected effects of treatment. Although its functions in PVL are not clear, the proinflammatory role of A_{2B}AR has been documented in asthma, and inflammatory bowel diseases. A_{2B} receptor activation induces an inflammatory response, for example by inducing the release of Interleukin (IL)-6 (Woodward et al., 2006). Consistent with reports, our experimental data also suggest that the agonist BAY60-6583 promotes

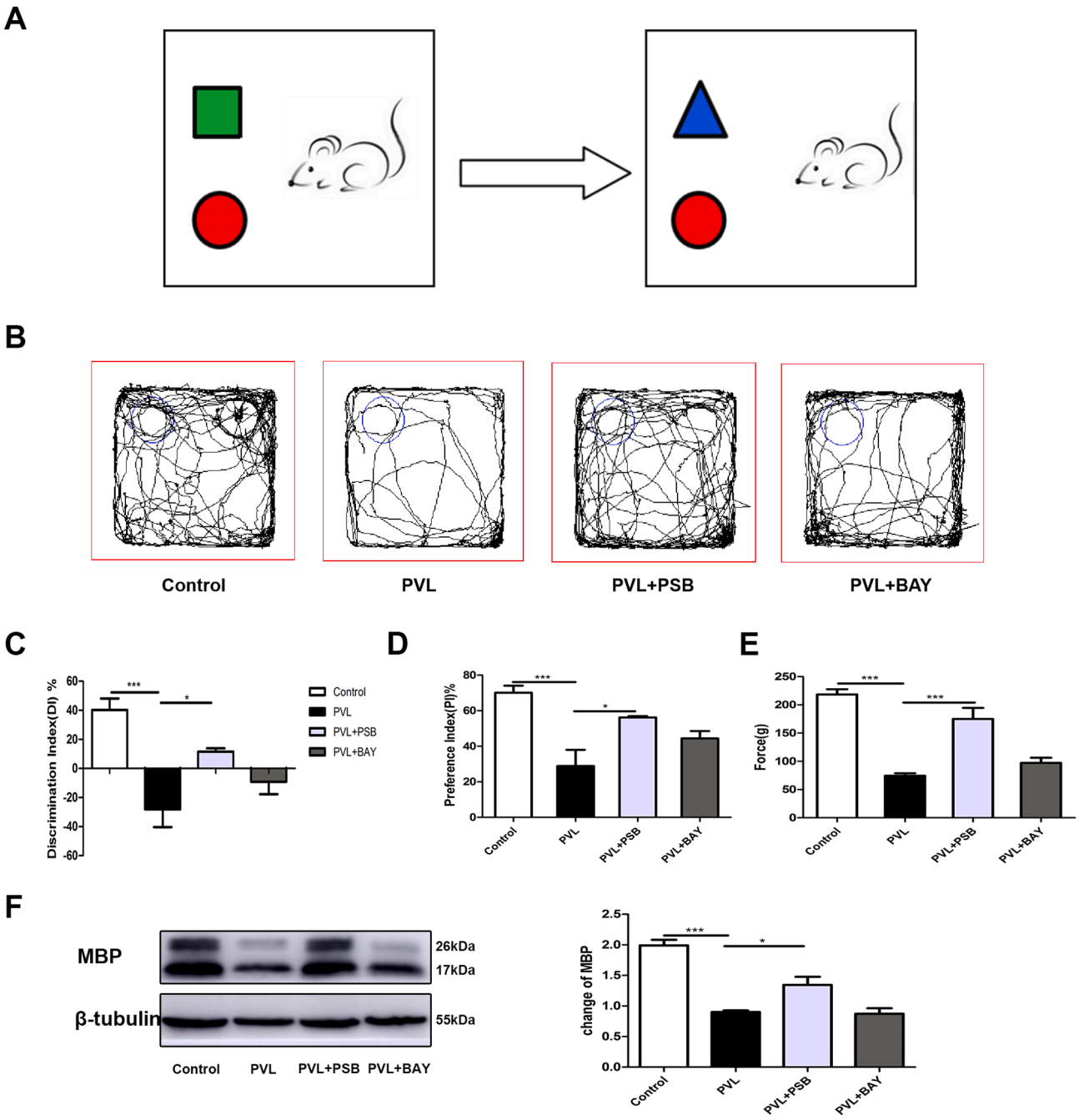

Fig. 6. Effects of A_{2B}AR inhibition on non-spatial learning, recognition, memory function and promoting myelination in PVL adult mice (P40). (A) Schematic diagram of the novel object recognition test. (B) Representative images of motion trajectories in the Control, PVL, PVL + PSB and PVL + BAY groups. (C) The DI values of the Control, PVL, PVL + PSB and PVL + BAY groups. (D) The PI values of the Control, PVL, PVL + PSB and PVL + BAY groups. (E) Grip strength test after PVL and A_{2B}AR treatment. (F) Representative western blotting images of MBP and the analysis of MBP protein expression levels in the cortex in of adult mice. All data are expressed as the mean ± SD (n = 6). $^{*}P < 0.05$ $^{**}P < 0.01$ and $^{***}P < 0.001$ vs. the PVL model group. PVL, Periventricular leukomalacia; PSB, A_{2B}AR selective antagonist PSB-603; BAY, A_{2B}AR selective agonist BAY60-6583.

the expression of some inflammatory factors and myelin-related proteins. Although the selectivity of this compound for the A_{2B}AR has been previously described (Su et al., 2020); any off-target or nonspecific side effects of BAY60-6583 or its metabolic derivatives should be considered. To circumvent these issues, this A_{2B}AR agonist may be a suitable and promising candidate for further investigation.

PVL is one of the predominant causes of infant neurological dysfunction, including cognitive dysfunction, myasthenia gravis, status epilepticus, and cerebral palsy (Hinz et al., 2014; Darashchonak et al., 2014). To verify whether PSB-603 could improve neurological deficits in PVL model mice, we bred the P9 PVL mice models to P40, during which the mice were injected with PSB-603 every other day. As a result, the strength of forelimb grip was significantly increased and muscular tension of limbs recovered after treated with PSB-603. The new object recognition tests indicated that inhibition of A_{2B}AR improved cognitive and neurosensory functional outcome. We also found that myelin loss remained in these P40 mice was significantly improved after PSB-603 treatment. It is known that neonatal demyelination is one of the major causes of neurological defects in adulthood. That means PSB-603 ameliorating neonatal PVL induced neurological deficits in P40 adult

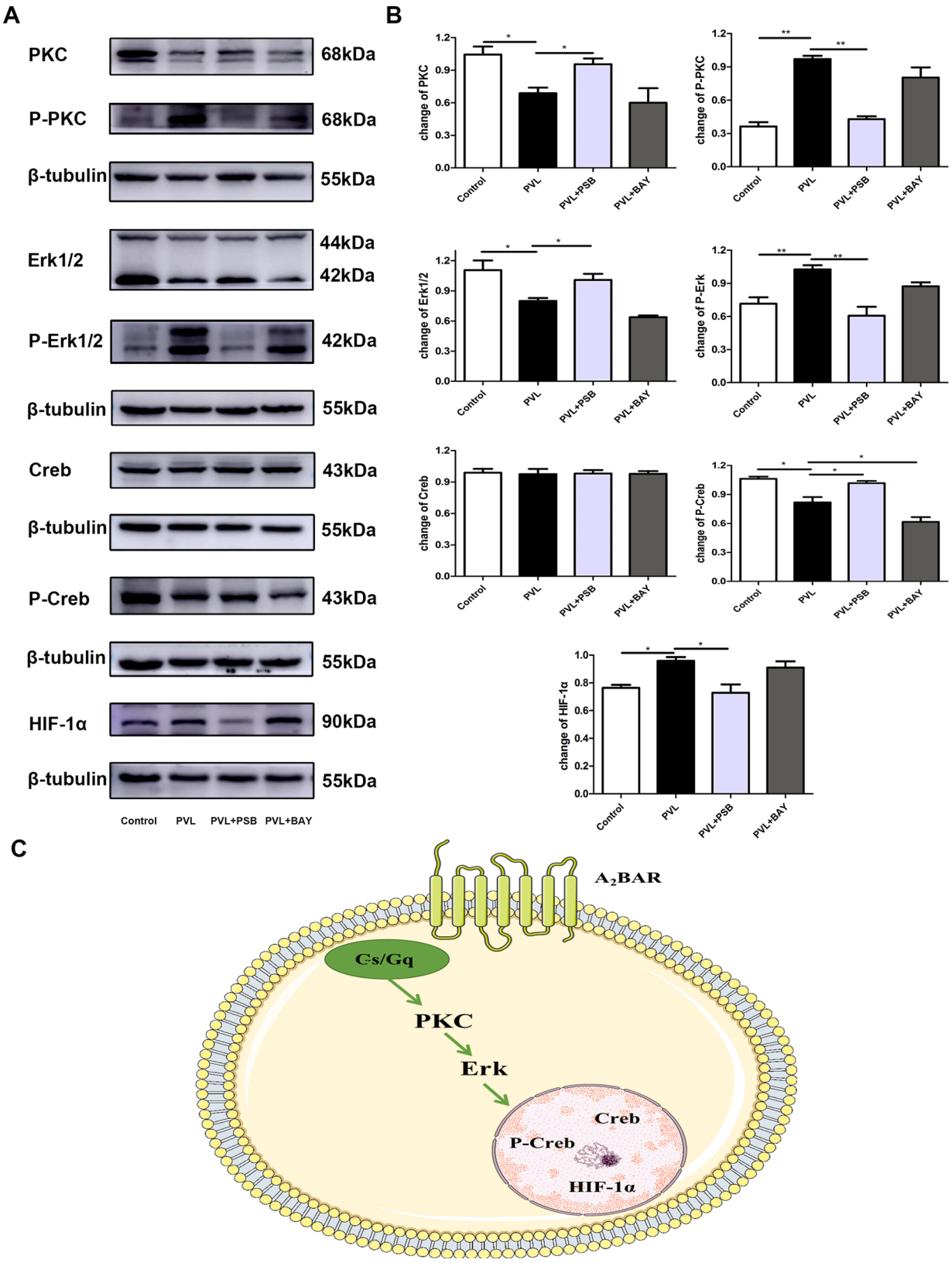

Fig. 7. $A_{2B}AR$ activated the PKC/Erk/Creb/HIF-1α signaling pathway in the brain via PVL. (A) Representative western blotting images of PKC, p-PKC, Erk, p-Erk, Creb, p-Creb and HIF-1α protein expression levels in the right cortex. (B) Effect of $A_{2B}AR$ on the PKC, Erk, p-Creb and HIF-1α protein activation of the PKC/Erk/Creb/HIF-1α signaling pathway after PVL. (C) Schematic diagram of $A_{2B}AR$ activated the PKC/Erk/Creb/HIF-1α signaling pathway in the brain via PVL. All data are expressed as the mean ± SD (n = 5). $^{*}P < 0.05$ and $^{**}P < 0.01$ vs. the PVL model group. PVL, Periventricular leukomalacia; PKC, protein kinase C; p-PKC, phosphor-protein kinase C; Erk, extracellular regulated protein kinases; p-Erk, phosphor-extracellular regulated protein kinases; Creb, cAMP-response element binding protein; p-Creb, phosphor-cAMP-response element binding protein; HIF-1α, hypoxia inducible factor-1α; PSB, $A_{2B}AR$ selective antagonists PSB-603; BAY, $A_{2B}AR$ selective agonists BAY60-6583.

mice may be due to the improvement of myelin loss.

Taken together, blocking $A_{2B}AR$ with its antagonist PSB-603 greatly ameliorated cerebral ischemic injury, suppressed neurons apoptosis, inhibited microglia activation and attenuated hypomyelination, while treatment with $A_{2B}AR$ agonist BAY60-6583 had no obvious effects. However, this lower efficacy may be attributed to the receptor expression levels, the local adenosine concentrations and potential constitutive receptor activity, making BAY60-6583 display a broad spectrum of efficacies ranging from full to partially agonistic and even antagonistic activity (Sun and Huang, 2016). In this study, the attempt was to inhibit the upregulated $A_{2B}AR$ in PVL, and PSB-603 was used as an inhibitor, while BAY60-6583 was used as a positive control. The results were promising as expected.

$A_{2B}AR$ is a typical GPCR structure and the second messenger pathway coupled with adenosine receptor subtypes, involving $A_{2B}AR$-Gq-phospholipase C (PLC)-protein kinase C (PKC), and the MAPK pathways (Borea et al., 2016). The expression of PKC has changed remarkably, which attracted our attention. The participation of the PKC/MAPK pathway in $A_{2B}AR$ signaling has been proposed by others (Li et al., 2021). When $A_{2B}AR$ is activated under pathological conditions, the activation of PKC triggers downstream signaling that can modulate the transcription of genes involved in inflammation and cell regulation, such as NFKB, Creb, and HIF-1α (Valera et al., 2008). LI Da Wei et al. found that PKC downstream protein Erk1/2 mRNA was obviously lower in the on middle cerebral artery of the prenatal hypoxia offspring (Wang et al., 2016). Consistent with our study, PKC phosphorylation and activation can increase the phosphorylation level of Erk1/2. The Erk activation can activate the Creb by activating the ribosomal S6 kinase, thus acting on the Cre and initiating the Cre-dependent transcription. In addition, Erk can also directly phosphorylate the transcription factor Creb, while Erk1/2 has a negative feedback on Creb (Shen et al., 2010). Some studies have found that 50 mg/kg/day bisphenol exposure in pregnant female mice can reduce the expression of p44/42MAPK and Creb phosphorylated protein in the hippocampus (Bot et al., 2012), which is consistent with the result of the decreased expression of p-Creb. In addition, we also noticed that the key regulators of adenosine - signaling are also direct targets of HIF-1α, which was significantly increased after exposure to PVL, because other researchers have suggested A_{2B} increases HIF-1α dependently under hypoxic conditions and might promote cell proliferation (Wen et al., 2015). In this study; we confirmed that PKC, Erk, p-Creb and HIF-1α are involved in the protective effects of $A_{2B}AR$ inhibition against brain injury in PVL mouse mode. However, PSB-603 played a more significant therapeutic role as a selective antagonist of $A_{2B}AR$.

4. Conclusion

In summary, the blockade of $A_{2B}AR$ with PSB-603 has neuroprotection effects against PVL mediated brain injury by alleviating inflammation, hypoxia and apoptosis and promoting OL maturation and remyelination through PKC/Erk/Creb/HIF-1α signaling pathway indicating that blocking $A_{2B}AR$ may represent a potential therapeutic strategy for hypoxia–ischemia induced PVL.

5. Material and methods

5.1. Animals

C57BL/6N mice (postnatal day 9, P9) were recruited from the laboratory animal center of Ningxia Medical University. The mice were kept in an environment with a temperature of 22 °C and an air humidity of 50%, with a light/dark cycle for 12 h, and free access to food and water. Experimental procedures were conducted in accordance with the National Institutes of Health guide for the care and use of Laboratory animals (NIH Publications No. 8023, revised 1978). The study was approved by the Animal Ethics and Welfare Committee of Ningxia Medical University (Reference number: IACUC-NYLAC-2020–034).

5.2. PVL mice model

The PVL model of neonatal mice adopted the classical Rice-Vannucci model to simulate the human hypoxic-ischemic encephalopathy (Tian et al., 2015). It was reported that mice had brain maturity at Day 9 after birth comparable to 36–40 weeks of old human fetuses (Liu et al., 2017). Therefore, in this study, 9-day-old mice were used. The mouse was anesthetized with isoflurane fixed in the supine position, and the right common carotid artery was permanently ligated with a cautery tip. The skin incision was sutured, and it was kept warm until fully awake, then returned to the home cage to recover for 1.5 h. Then it was put in the hypoxia box (8% O_2 + 92% N_2) for 80 min to induce Hypoxia-Ischemia (H-I). Finally, 15 μL lipopolysaccharide (LPS, 1 mg/kg) was injected into the abdominal cavity of the mouse. Mice in the sham group were only freed the right common carotid artery and injected normal saline (15 μL) into the abdominal cavity.

5.3. Group design of experiments

Eighty P9 C57BL/6N mice were randomly assigned to one of the four experimental groups (20 mice per group): Control group: mice were intraperitoneally injected with an equal volume of saline for 6 days. Model mice group with Periventricular leukomalacia (PVL): hypoxic-ischemic insults and intraperitoneally injected with LPS 1 mg/kg daily. PVL with $A_{2B}AR$ selective antagonist PSB-603 group (PVL + PSB): after PVL induction, mice were intraperitoneally injected with PSB-603 25 μg/kg daily for 6 consecutive days (from P9 to P14). PVL with $A_{2B}AR$ selective agonist BAY60-6583 group (PVL + BAY): after PVL induction, mice were intraperitoneally injected with BAY60-6583 80 μg/kg daily for 6 consecutive days (from P9 to P14). The average daily body weight per mouse was monitored. After 14 days, brain tissues were harvested. Prior to euthanization, the P40 mice were subjected to behavioral tests. According to the literature and the previous research of the research group, we determined the optimal dose and scheduling for use BAY 60-6583 (Kaji et al., 2014; Alnouri et al., 2015; Niatsetskaya et al., 2020), and PSB-603 (Kaji et al., 2014; Alnouri et al., 2015) (Tocris Bioscience, Bristol, UK). The doses of the BAY 60-6583 and PSB-603 used in this study were equal to or less than those used in the literature, which reported no significant effect on hemodynamics.

5.4. TTC staining

At Day 14 of post-hypoxic-ischemic insult, mice were anesthetized with 4% chloral hydrate through intraperitoneal injection. The infarct staining of the brain tissue sections was performed with 2,3,5-triphenyltetrazolium chloride (TTC) (Sigma-Aldrich, Hamburg Germany). The brain was cut into 2 mm coronal sections and placed in an oven with 2% TTC solution at 37 °C, and stained in the dark for 15–30 min to evaluate the infarct size. Image-Pro Plus 6.0 software was used to quantify the infarct area as a proportion of the total area.

5.5. Immunofluorescence imaging

At Day 14 of post-hypoxic-ischemic insult, mice were deeply anesthetized with 4% chloral hydrate and transcardially perfused with 4% paraformaldehyde. Brains were collected and postfixed with 4% paraformaldehyde overnight, then these tissues were dehydrated in 30% sucrose in 0.01 M PBS. Brains were embedded in optimal cutting temperature compound (O.C.T. Compound, USA) and then sliced coronally (25 μm) on a cryostat microtome (MS 1850, Leica, Wetzlar, Germany). Brain tissue was sliced in the area containing the corpus callosum. All brain slices were obtained from independent experiments, and analysis was performed from brain slices at similar anatomical locations. Subsequently, the sections were blocked with 5% bovine serum albumin

(BSA), 0.1% normal goat serum (NGS) and 0.2% Triton X-100 at room temperature for 1 h, and then incubated with primary antibodies at 4 °C overnight. Primary antibodies included: rabbit anti-Olig2 antibody (1:200, Abcam, Cat: ab109186), rabbit anti-CC-1 antibody (1:200, Calbiochem, Cat: No.OP80), rat anti-MBP antibody (1:1000, Abcam, Cat: ab7349), rabbit anti Iba1 antibody (1:250, Abcam, Cat:019-19741). Then the brain slices were washed three times with phosphate-buffered saline (PBS) for 10 min each time, and the slices were incubated with fluorescently-labeled secondary antibodies for 2 h at room temperature in the dark, and finally mounted with DAPI-containing mounting tablets. Secondary antibodies included: AlexaFluor-488 or AlexaFluor-568 secondary antibodies against rabbit, mouse or rat (1:200; Abbkine; Cat:A23420; Cat:A23240-1; Cat:A23210). The images were observed under a fluorescence microscope, and the number of positive cells in the right cortex and corpus callosum was analyzed with Image-Pro Plus 6.0 software.

5.6. Histopathological analysis

At Day 14 of post-hypoxic-ischemic insult, mice were anesthetized with 4% chloral hydrate (intraperitoneal injection) and transcardiac perfusion of 0.9% normal saline and 4% paraformaldehyde was performed. Finally, the brain was collected and fixed at 4 °C with 4% paraformaldehyde overnight. The fixed brain was embedded in paraffin and 5 μm sections were obtained. Sections obtained from each brain were dewaxed with xylene, progressively dehydrated with ethanol, and subsequently stained with hematoxylin and eosin (H&E) staining (Cat: DH0006; LEAGENE®; http://www.leagene.com) and Nissl staining (Cat:C0117; www.beyotime.com). The morphological changes of the necrotic cells in right cortex region were observed with a microscope.

5.7. Western blotting

The brain tissues were rinsed with PBS, lysed on ice with RIPA lysis buffer (Keygentec, China) containing protease and phosphatase inhibitor (100 μM), and the brain homogenates were centrifuged for 15 min (12,000 rpm, 4 °C) and the supernatants were collected in separate tubes. The protein concentration was determined using a BCA protein assay (Cat: KGP2100, Key GEN BioTECH). An equal amount of 30μg of total protein in each sample was transferred to the PVDF membrane (0.45 μm, Immobilon-P, Millipore), blocked with 5% milk, and incubated with primary antibodies anti-MBP (1:1000, Abcam, Cat:ab7349), anti-PKC (1:1000, Abcam, Cat:ab75991), anti-p-PKC (1:1000, ABclonal, Cat:AP0520), anti-HIF-1α (1:1000, Abcam, Cat:ab216842), anti-Creb (1:1000, ABclonal, Cat:A11064), anti-p-Creb (1:1000, ABclonal, Cat: AP0903), anti-Erk1/2 (1:1000, Wanlei, Cat:WL01864), anti-p-Erk1/2 (1:1000, Wanlei, Cat:WLP512), anti-Iba1 (1:1000, Cat:019-19741), anti-Caspase-3 (1:1000, Abbkine, Cat:#ABP0135), anti-NeuN (1:1000, Abcam, Cat:ab104224) overnight at 4 °C, then incubated with the appropriate HRP-conjugated secondary antibody (1:5000, Abbkine, Cat: #A21020, Cat:#A21040, Cat:#A21010). After incubation at room temperature for 1 h, chemiluminescent detection was performed and the protein bands were captured and analyzed using an imaging system that quantified using Image J.

5.8. Enzyme-linked immunosorbent assay (ELISA)

Levels of interleukin (IL)-6, IL-1β, IL-10 and tumor necrosis factor-α (TNF-α) in the brain tissue supernatant were detected by ELISA kits (JINGMEI BIOLOGICALTECHNOLOGY, JIANGSU) according to the manufacturer's instructions. In short, the blood was washed off with ice-cold PBS (pH = 7.4). After washing, the homogenate was made with an automatic sample cryo-grinding instrument at 4 °C then centrifuged at 2000–3000 rpm for 20 min to remove the supernatant. The blank well was set as zero, a spectrophotometer was used to read the absorbance at 450 nm, and then the equation generated by the standard curve was used to calculate the brain sample levels.

5.9. Behavioral tests

A series of behavioral tests including the Olfactory discrimination test, the Grip strength test, and the New object recognition test were performed to identify the major dysfunctions in the mice. All mice were fed at a 12 h /12 h cycle day and night. In order to prevent the mice from smelling the unpleasant odor, the behavioral equipment was wiped with 30% ethanol before and after each test.

5.9.1. Olfactory discrimination test

The experiment was carried out as described in the previous literature (Niatsetskaya et al., 2020). The mice on the 14th day after birth were selected for the olfactory discrimination test. In a standard plastic squirrel cage, one side was filled with used bedding and the other side was filled with unused bedding. A P14 mouse was placed in the middle position at a distance equal to the length of the baby mouse's body. The time it took for the pups to enter the bedding area was recorded. The longest time was set to enter the bedding area as 60 s. If the pup failed to enter the bedding area, the maximum time would be calculated. The experiment was repeated 3 times for each pup.

5.9.2. Grip strength test

Grip strength test forelimb grip strength was assessed using the YLS12A grip strength instrument, which was used to evaluate the grip strength of the mouse forelimbs on the 40th day after birth. The tail of the mouse was gently lift, its forelimbs were placed on the grid and pulled back, and the instrument automatically recorded the tensile force value. The experiment was repeated three times for each mouse and used for statistical analysis.

5.9.3. Novel object recognition test

The experiment was carried out as described in the previous literature (Grayson et al., 2015). In short, the experimental device was composed of a white polyethylene plastic square open area (25 × 25 × 40 cm) box. The three objects used for identification were 5.8 cm high, with a cylinder (red), a cube (green) and a pyramid (blue). The day before the test, the P40 mice were allowed to explore the box for 10 min without any objects. The formal test was carried out 2 exploratory tests with an interval of 2 h. In the first exploratory experiment, two rectangular plastic objects (A and B) were placed 8 cm away from the wall of the instrument, and a mouse was randomly selected and placed in the box and allowed to explore for 10 min. In the second exploratory experiment, one of the rectangular objects (B) was replaced with a cylinder (C), and the same mouse was put in again. The exploration time of each mouse familiar with the object (F = A + B) and familiar with the new object (N = A + C) was manually recorded. The discrimination index (DI) was calculated as N-F/(N + F) × 100%. The discrimination index (DI), which the DI value was >50% if the mice showed tendencies of exploring novel objects, was calculated by N − F/(N + F) × 100% for intergroup comparisons. The preference index (PI), which reflected the ability of mice to explore new objects, was calculated by N/(N + F) × 100% for intergroup comparisons.

5.10. Statistical analysis

The SPSS software (IBM SPSS Version 22, Chicago, IL, USA) and GraphPad 8.0 software (GraphPad Software, Inc.) program was used for performing the statistical analysis. Each experiment was performed using 3–5 mice and repeated at least three times. The data was expressed using the means ± standard deviation. The difference between multiple comparisons was analyzed using two-way analysis of variance and Tukey's multiple comparison test. Student's *t*-test (two-tailed) was used to evaluate the difference between the two groups. If the P value < 0.05, the data was considered to be statistically significant.

CRediT authorship contribution statement

Junyan Wang: Conceptualization, Methodology, Software, Writing – original draft, Investigation. **Dan Wang:** Methodology, Conceptualization, Investigation. **Xiaomin Zheng:** Conceptualization, Methodology, Software. **Yunhong Li:** Methodology, Software. **Yilu Li:** Methodology, Visualization. **Teng Ma:** Visualization. **Jinxia Li:** Methodology, Visualization. **Jinping Sun:** Supervision. **Yin Wang:** Funding acquisition, Project administration, Supervision, Writing – review & editing. **Quanrui Ma:** Funding acquisition, Project administration, Supervision.

Declaration of Competing Interest

The authors declare that they have no known competing financial interests or personal relationships that could have appeared to influence the work reported in this paper.

Acknowledgements

This work was supported by the National Natural Science Foundation of China (grant nos. 82060223, 32160192 and 31360240), Ningxia Natural Science Foundation (grant nos. 2020AAC03143, 2020AAC03150, 2021AAC03372 and NZ17072), Ningxia key research and development program (2021BEG03097) and CAS "Light of West China" Program (grant no. XAB2017AW05).

References

Aherne, C.M., Kewley, E.M., Eltzschig, H.K., 2011. The resurgence of A2B adenosine receptor signaling. Biochim. Biophys. Acta 1808 (5), 1329–1339.

Alnouri, M.W., Jepards, S., Casari, A., Schiedel, A.C., Hinz, S., Müller, C.E., 2015. Selectivity is species-dependent: characterization of standard agonists and antagonists at human, rat, and mouse adenosine receptors. Purinerg Signal 11 (3), 389–407.

Back, S.A., 2017. White matter injury in the preterm infant: pathology and mechanisms. Acta Neuropathol. 134 (3), 331–349.

Borea, P.A., Gessi, S., Merighi, S., Varani, K., 2016. Adenosine as a multi-signalling guardian angel in human diseases: when, where and how does it exert its protective effects? Trends Pharmacol. Sci. 37 (6), 419–434.

Bot, I., de Vries, H., Korporaal, S.J.A., Foks, A.C., Bot, M., van Veldhoven, J., ter Borg, M. N.D., van Santbrink, P.J., van Berkel, T.J.C., Kuiper, J., Ijzerman, A.P., 2012. Adenosine A2B receptor agonism inhibits neointimal lesion development after arterial injury in apolipoprotein E-deficient mice. Arterioscler. Thromb. Vasc. Biol. 32 (9), 2197–2205.

Chang, K.-J., Redmond, S.A., Chan, J.R., 2016. Remodeling myelination: implications for mechanisms of neural plasticity. Nat. Neurosci. 19 (2), 190–197.

Coppi, E., Cherchi, F., Fusco, I., Dettori, I., Gaviano, L., Magni, G., Catarzi, D., Colotta, V., Varano, F., Rossi, F., Bernacchioni, C., Donati, C., Bruni, P., Pedata, F., Cencetti, F., Pugliese, A.M., 2020. Adenosine A2B receptors inhibit K(+) currents and cell differentiation in cultured oligodendrocyte precursor cells and modulate sphingosine-1-phosphate signaling pathway. Biochem. Pharmacol. 177, 113956. https://doi.org/10.1016/j.bcp.2020.113956.

Darashchonak, N., Koepsell, B., Bogdanova, N., von Versen-Höynck, F., 2014. Adenosine A2B receptors induce proliferation, invasion and activation of cAMP response element binding protein (CREB) in trophoblast cells. BMC Pregnancy Childb. 14 (1), 2.

Effendi, W.I., Nagano, T., Kobayashi, K., Nishimura, Y., 2020. Focusing on adenosine receptors as a potential targeted therapy in human diseases. Cells-Basel 9 (3), 785. https://doi.org/10.3390/cells9030785.

Franklin, R.J.M., ffrench-Constant, C., 2017. Regenerating CNS myelin — from mechanisms to experimental medicines. Nat. Rev. Neurosci. 18 (12), 753–769.

Fredholm, B.B., IJzerman, A.P., Jacobson, K.A., Linden, J., Müller, C.E., 2011. International union of basic and clinical pharmacology. LXXXI. Nomenclature and classification of adenosine receptors—an update. Pharmacol. Rev. 63 (1), 1–34.

Gnad, T., Navarro, G., Lahesmaa, M., Reverte-Salisa, L., Copperi, F., Cordomi, A., Naumann, J., Hochhäuser, A., Haufs-Brusberg, S., Wenzel, D., Suhr, F., Jespersen, N. Z., Scheele, C., Tsvilovskyy, V., Brinkmann, C., Rittweger, J., Dani, C., Kranz, M., Deuther-Conrad, W., Eltzschig, H.K., Niemi, T., Taittonen, M., Brust, P., Nuutila, P., Pardo, L., Fleischmann, B.K., Blüher, M., Franco, R., Bloch, W., Virtanen, K.A., Pfeifer, A., 2020. Adenosine/A2B receptor signaling ameliorates the effects of aging and counteracts obesity. Cell Metab. 32 (1), 56–70.e7.

Grayson, B., Leger, M., Piercy, C., Adamson, L., Harte, M., Neill, J.C., 2015. Assessment of disease-related cognitive impairments using the novel object recognition (NOR) task in rodents. Behav. Brain Res. 285, 176–193.

Han, Q., Lin, Q., Huang, P., Chen, M., Hu, X., Fu, H., He, S., Shen, F., Zeng, H., Deng, Y., 2017. Microglia-derived IL-1β contributes to axon development disorders and synaptic deficit through p38-MAPK signal pathway in septic neonatal rats. J. Neuroinflamm. 14 (1) https://doi.org/10.1186/s12974-017-0805-x.

Harmony, T., 2021. Early diagnosis and treatment of infants with prenatal and perinatal risk factors for brain damage at the neurodevelopmental research unit in Mexico. Neuroimage 235, 117984. https://doi.org/10.1016/j.neuroimage.2021.117984.

Haskó, G., Linden, J., Cronstein, B., Pacher, P., 2008. Adenosine receptors: therapeutic aspects for inflammatory and immune diseases. Nat. Rev. Drug Discov. 7 (9), 759–770.

Haynes, R.L., van Leyen, K., 2013. 12/15-Lipoxygenase expression is increased in oligodendrocytes and microglia of periventricular leukomalacia. Dev. Neurosci.-Basel. https://doi.org/10.1159/000350230.

Hinz, S., Lacher, S.K., Seibt, B.F., Müller, C.E., 2014. BAY60-6583 acts as a partial agonist at adenosine A2B receptors. J. Pharmacol. Exp. Ther. 349 (3), 427–436.

Kaji, W., Tanaka, S., Tsukimoto, M., Kojima, S., 2014. Adenosine A(2B) receptor antagonist PSB603 suppresses tumor growth and metastasis by inhibiting induction of regulatory T cells. J. Toxicol. Sci. 39 (2), 191–198.

Kwon, J.H., Lee, J., Kim, J., Jo, Y.H., Kirchner, V.A., Kim, N., Kwak, B.J., Hwang, S., Song, G.W., Lee, S.G., Yoon, Y.I., Park, G.C., Tak, E., 2019. HIF-1alpha regulates A2B adenosine receptor expression in liver cancer cells. Exp. Ther. Med. 18 (6), 4231–4240.

Li, D.W., Bo, L., Tu, Q., Zhou, A.W., Shi, L.L., Yang, X.J., Mao, C.P., 2021. Prenatal hypoxia altered angiotensin II-mediated vasoconstrictions viaPKC/ERK/ROCK pathways and potassium channels in rat offsrping middle cerebral artery. Biomed. Environ. Sci. 34 (3), 250–255.

Lindemann, M., Moldovan, R., Hinz, S., Deuther-Conrad, W., Gündel, D., Dukic-Stefanovic, S., Toussaint, M., Teodoro, R., Juhl, C., Steinbach, J., Brust, P., Müller, C. E., Wenzel, B., 2020. Development of a radiofluorinated adenosine A2B receptor antagonist as potential ligand for PET imaging. Int. J. Mol. Sci. 21 (9), 3197.

Liu, S., Xin, D., Wang, L., Zhang, T., Bai, X., Li, T., Xie, Y., Xue, H., Bo, S., Liu, D., Wang, Z., 2017. Therapeutic effects of L-Cysteine in newborn mice subjected to hypoxia-ischemia brain injury via the CBS/H2S system: Role of oxidative stress and endoplasmic reticulum stress. Redox Biol. 13, 528–540.

Mao, F.-X., Chen, H.-J., Qian, L.-H., Buzby, J.S., 2020. GPR17 plays a role in ischemia-induced endogenous repair of immature neonatal cerebral White matter. Brain Res. Bull. 161, 33–42.

Miron, V.E., Boyd, A., Zhao, J.-W., Yuen, T.J., Ruckh, J.M., Shadrach, J.L., van Wijngaarden, P., Wagers, A.J., Williams, A., Franklin, R.J.M., ffrench-Constant, C., 2013. M2 microglia and macrophages drive oligodendrocyte differentiation during CNS remyelination. Nat. Neurosci. 16 (9), 1211–1218.

Montalbán del Barrio, I., Penski, C., Schlahsa, L., Stein, R.G., Diessner, J., Wöckel, A., Dietl, J., Lutz, M.B., Mittelbronn, M., Wischhusen, J., Häusler, S.F.M., 2016. Adenosine-generating ovarian cancer cells attract myeloid cells which differentiate into adenosine-generating tumor associated macrophages – a self-amplifying, CD39- and CD73-dependent mechanism for tumor immune escape. J. ImmunoTher. Cancer 4 (1). https://doi.org/10.1186/s40425-016-0154-9.

Neumann, B., Segel, M., Chalut, K.J., Franklin, R.J.M., 2019. Remyelination and ageing: Reversing the ravages of time. Mult. Scler. 25 (14), 1835–1841.

Niatsetskaya, Z., Sosunov, S., Stepanova, A., Goldman, J., Galkin, A., Neginskaya, M., Pavlov, E., Ten, V., 2020. Cyclophilin D–dependent oligodendrocyte mitochondrial ion leak contributes to neonatal white matter injury. J. Clin. Invest. 130 (10), 5536–5550.

Ortega, S.B., Kong, X., Venkataraman, R., Savedra, A.M., Kernie, S.G., Stowe, A.M., Raman, L., 2016. Perinatal chronic hypoxia induces cortical inflammation, hypomyelination, and peripheral myelin-specific T cell autoreactivity. J. Leukoc. Biol. 99 (1), 21–29.

Rumajogee P, Bregman T, Miller SP, Yager JY, Fehlings MG. Rodent hypoxia–ischemia models for cerebral palsy research: a systematic review. Front. Neurol. 2016, **7**.

Salsoso, R., Mate, A., Toledo, F., Vázquez, C.M., Sobrevia, L., 2021. Insulin requires A2B adenosine receptors to modulate the L-arginine/nitric oxide signalling in the human fetoplacental vascular endothelium from late-onset preeclampsia. Biochim. Biophys. Acta Mol. Basis Dis. 1867 (1), 165993. https://doi.org/10.1016/j.bbadis.2020.165993.

Schulte, G., Fredholm, B.B., 2003. Signalling from adenosine receptors to mitogen-activated protein kinases. Cell. Signal. 15 (9), 813–827.

Shen, Y., Plane, J.M., Deng, W., 2010. Mouse models of periventricular leukomalacia. J. Visualized Exp. 39.

Sherwin, C., Fern, R., 2005. Acute lipopolysaccharide-mediated injury in neonatal white matter glia: role of TNF-α, IL-1β, and calcium. J. Immunol. 175 (1), 155–161.

Simon, C., Götz, M., Dimou, L., 2011. Progenitors in the adult cerebral cortex: cell cycle properties and regulation by physiological stimuli and injury. Glia 59 (6), 869–881.

Su, B.-H., Lin, H.-Y., Chiu, H.-Y., Tsai, M.-L., Chen, Y.-T., Lu, I.-C., 2020. Therapeutic strategy of patent ductus arteriosus in extremely preterm infants. Pediatr. Neonatol. 61 (2), 133–141.

Sun, Y., Huang, P., 2016. Adenosine A2B receptor: from cell biology to human diseases. Front. Chem. 4.

Tian, Y., Piras, B.A., Kron, I.L., French, B.A., Yang, Z., 2015. Adenosine 2B receptor activation reduces myocardial reperfusion injury by promoting anti-inflammatory macrophages differentiation via PI3K/Akt pathway. Oxid. Med. Cell Longev 2015, 1–8.

Valera, E., Sanchezmartin, F., Ferrermontiel, A., Messeguer, A., Merino, J., 2008. NMDA-induced neuroprotection in hippocampal neurons is mediated through the protein kinase A and CREB (cAMP-response element-binding protein) pathway. Neurochem. Int. 53 (5), 148–154.

van der Hoeven, D., Wan, T.C., Gizewski, E.T., Kreckler, L.M., Maas, J.E., Van Orman, J., Ravid, K., Auchampach, J.A., 2011. A role for the low-affinity A2B adenosine

receptor in regulating superoxide generation by murine neutrophils. J. Pharmacol. Exp. Ther. 338 (3), 1004–1012.
Verkhratsky, A., Burnstock, G., 2014. Biology of purinergic signalling: its ancient evolutionary roots, its omnipresence and its multiple functional significance. BioEssays 36 (7), 697–705.
Wang, C., Li, Z., Han, H., Luo, G., Zhou, B., Wang, S., Wang, J., 2016. Impairment of object recognition memory by maternal bisphenol A exposure is associated with inhibition of Akt and ERK/CREB/BDNF pathway in the male offspring hippocampus. Toxicology 341-343, 56–64.
Wei, W., Du, C., Lv, J., Zhao, G., Li, Z., Wu, Z., Haskó, G., Xie, X., 2013. Blocking A2B adenosine receptor alleviates pathogenesis of experimental autoimmune encephalomyelitis via inhibition of IL-6 production and Th17 differentiation. J. Immunol. 190 (1), 138–146.
Wen, J., Wang, B., Du, C., Xu, G., Zhang, Z., Li, Y.i., Zhang, N., 2015. A2B adenosine receptor agonist improves erectile function in diabetic rats. Tohoku J. Exp. Med. 237 (2), 141–148.
Woodward, L.J., Anderson, P.J., Austin, N.C., Howard, K., Inder, T.E., 2006. Neonatal MRI to predict neurodevelopmental outcomes in preterm infants. New Engld. J. Med. 355 (7), 685–694.